JOURNAL OF THERMOPHYSICS AND HEAT TRANSFER
Vol. 11, No. 2, April–June 1997

Analysis of Discrete Ordinates Method with Even Parity Formulation

J. Liu,* H. M. Shang,† and Y. S. Chen‡
Engineering Sciences, Inc., Huntsville, Alabama 35802
and
T. S. Wang§
NASA Marshall Space Flight Center, Huntsville, Alabama 35812

The even parity formulation (EPF) of the discrete ordinates method (DOM) is used to simulate radiative heat transfer in two-dimensional enclosures containing an absorbing–emitting and scattering medium. The discrete ordinates equations for the EPF are second-order differential equations and they are spatially discretized using a second-order central difference scheme. At the boundary, a higher-order upwind scheme is employed to prevent solution instability and minimize errors. The matrix solver of the discretized equations is based on a preconditioned conjugate gradients method. To investigate the accuracy and efficiency of the EPF of the DOM, several two-dimensional benchmark problems with an absorbing–emitting and scattering medium enclosed by gray walls are considered. By taking an appropriate numerical treatment, the numerical results from the EPF appear to compare favorably with other available solutions. However, the even parity solution usually requires more CPU time and iterations to converge in comparison with the conventional DOM, especially for the case with a small optical thickness. This work indicates that the EPF of the DOM may be not as robust as the conventional DOM.

Nomenclature

E = emissive power
F = first variable in the EPF
G = second variable in the EPF
G_r = incident radiation
H = enclosure height
I = radiative intensity
I_b = blackbody radiative intensity
i, j = volume index numbers
L = enclosure length
M = total discrete direction numbers over a solid angle of 2π
MX = maximum volume index number in x direction
MY = maximum volume index number in y direction
m = discrete direction number
$\boldsymbol{n}$ = surface normal vector
Q_w = net radiative wall heat flux
q = irradiation
$\boldsymbol{r}$ = location vector
w = weight of a discrete direction
x, y = physical coordinates
ε = wall emissivity
κ = absorption coefficient
μ, ξ = direction cosines
σ = scattering coefficient
Φ = scattering phase function
Ω = direction vector

Introduction

RADIATION heat transfer is one of the major modes of heat transfer in boilers, furnaces, rocket engines, and other high-temperature combustion systems. An accurate prediction of radiation is very important for the design of these systems. In the last several decades, many methods have been developed for predicting radiative heat transfer in combustion systems. They include the zone method, Monte Carlo method, flux method, discrete ordinates method (DOM), etc. The zone method has the advantage of achieving very accurate solutions, often termed as exact. However, it has difficulty accounting for the scattering and spectral information of gases, and its applications are restricted to relatively simple geometries since the evaluation of direct exchange areas is too cumbersome for complicated geometries. Similar to the zone method, the Monte Carlo method can predict radiative heat transfer accurately, but its execution is very time consuming for complicated problems. The flux method was once a very popular method in accounting for radiation effects in combustion systems because of its easy formulation and compatible numerical algorithms with those for solving fluid transport equations. However, this method approximates angular intensity distribution along only four (two-dimensional) or six (three-dimensional) directions, and thus, accuracy is limited. Currently, one of the most widely used methods in combustion systems is the DOM.

In the DOM, the radiative transfer equation (RTE) is directly solved numerically along discrete directions that approximate the angular intensity distribution. As a result, the DOM is relatively easy to code, it provides accurate results by using higher-order approximations, it can account for spectral absorption by gases and scattering by particles, and it is compatible with numerical algorithms for solving transport equations.[1] Currently, there are two types of RTE used with DOM. One is the conventional RTE, which is a first-order differential equation, and the other is the even parity formulation (EPF), which is a second-order differential equation. While most work on the DOM is focused on the conventional RTE, application of the EPF in the DOM has received attention only recently in the heat transfer community.

The EPF of the DOM was originally applied in neutron transport applications.[2] Song and Park[3] are the first to apply this formulation in radiative heat transfer problems. They

Received May 24, 1996; revision received Aug. 24, 1996; accepted for publication Dec. 3, 1996.

*Research Scientist. Member AIAA.
†Senior Research Scientist. Member AIAA.
‡President and Chief Technical Officer. Senior Member AIAA.
§Team Leader, Computational Analysis Team, Fluid Dynamics Analysis Branch. Member AIAA.

transformed the conventional RTE into a second-order differential equation with integral scattering terms and investigated two problems to demonstrate the solution accuracy. Fiveland and Jessee[4,5] formulated the conventional RTE and the EPF with the finite element method and compared the even parity solution with other solutions for different cases. Their results indicated that the accuracy of the even parity predictions degraded as the optical thickness and wall emissivity were increased. Koch et al.[6] applied the EPF in a body-fitted coordinate system. Their study mainly focused on the effects of nonorthogonal grids. It was found that directional biasing and ray effects still existed in the even parity solution.

Because of the completely different mathematical structures, some numerical features in the EPF of the DOM are quite different from those in the conventional DOM, and their examination is necessary for determining the application of the EPF. In this paper, the accuracy and efficiency in the numerical solution from the EPF will be investigated by considering several two-dimensional benchmark problems. This work represents another effort to explore the unique numerical features of the EPF. In the next section, the even parity RTE is formulated first. After that, numerical analysis is conducted on the RTE, which includes derivation and discretization of the discrete ordinates equations and discussion of the solution method. Finally, the problems considered in Refs. 3–5 are revisited and the accuracy and computational efficiency of the even parity solution are discussed.

General Formulation

Consider the RTE for a two-dimensional rectangular enclosure with the L and H as shown in Fig. 1. The balance of energy passing in a specified direction Ω through a small differential volume in an absorbing–emitting and scattering gray medium can be written as

$$(\Omega\cdot\nabla)I(\boldsymbol{r},\Omega) = -(\kappa+\sigma)I(\boldsymbol{r},\Omega) + \kappa I_b(\boldsymbol{r}) + \frac{\sigma}{4\pi}\int_{\Omega'=4\pi} I(\boldsymbol{r},\Omega')\Phi(\Omega'\to\Omega)\,\mathrm{d}\Omega' \tag{1}$$

where $I(\boldsymbol{r},\Omega)$ is the radiative intensity, which is a function of position and direction; $I_b(\boldsymbol{r})$ is the blackbody radiative intensity at the temperature of the medium; and $\Phi(\Omega'\to\Omega)$ is the scattering phase function.

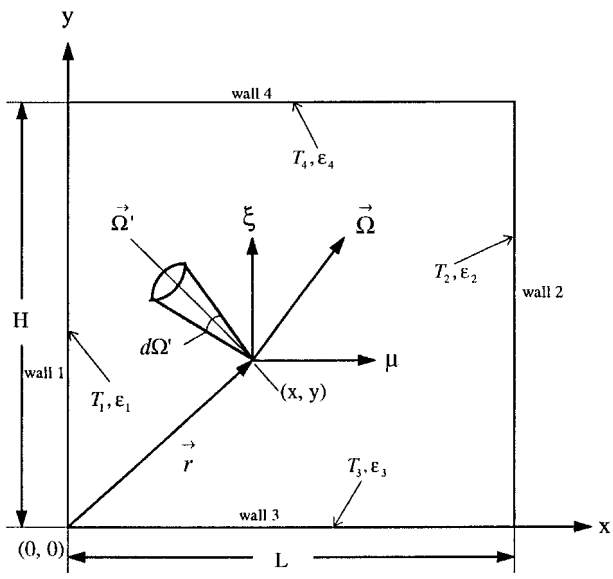

Fig. 1 Schematic of rectangular geometry.

If the wall bounding the medium is assumed gray and emits and reflects diffusely, then the radiative boundary condition for Eq. (1) is given by

$$I(\boldsymbol{r}_w,\Omega^+) = \varepsilon I_b(\boldsymbol{r}_w) + \frac{(1-\varepsilon)}{\pi}q(\boldsymbol{r}_w) \tag{2a}$$

with

$$q(\boldsymbol{r}_w) = \int_{\boldsymbol{n}\cdot\Omega^-<0} I(\boldsymbol{r}_w,\Omega^-)\left|\boldsymbol{n}\cdot\Omega^-\right|\,\mathrm{d}\Omega^- \tag{2b}$$

where Ω^+ and Ω^- denote the leaving and arriving radiative intensity directions, respectively, and $q(\boldsymbol{r}_w)$ is the irradiation on the wall.

The even parity form of the RTE is derived by considering opposite directions Ω and $-\Omega$, and by defining the following quantities:

$$F(\boldsymbol{r},\Omega) = I(\boldsymbol{r},\Omega) + I(\boldsymbol{r},-\Omega) \tag{3}$$

$$G(\boldsymbol{r},\Omega) = I(\boldsymbol{r},\Omega) - I(\boldsymbol{r},-\Omega) \tag{4}$$

Equation (1) can be written for the direction Ω and $-\Omega$. Adding and subtracting the resulting equations using Eqs. (3) and (4) leads to the following equations for the variables F and G:

$$(\Omega\cdot\nabla)F(\boldsymbol{r},\Omega) = -(\kappa+\sigma)G(\boldsymbol{r},\Omega) + \frac{\sigma}{4\pi}\int_{\Omega'=2\pi} G(\boldsymbol{r},\Omega')[\Phi(\Omega'\to\Omega)-\Phi(\Omega'\to-\Omega)]\,\mathrm{d}\Omega' \tag{5}$$

$$(\Omega\cdot\nabla)G(\boldsymbol{r},\Omega) = -(\kappa+\sigma)F(\boldsymbol{r},\Omega) + 2\kappa I_b(\boldsymbol{r}) + \frac{\sigma}{4\pi}\int_{\Omega'=2\pi} F(\boldsymbol{r},\Omega')[\Phi(\Omega'\to\Omega)+\Phi(\Omega'\to-\Omega)]\,\mathrm{d}\Omega' \tag{6}$$

It should be noted that the integrations in the previous two equations are made only over 2π solid angles. For the sake of simplicity, only isotropic scattering is considered. The derivation of the formulation for anisotropic scattering is tedious and interested readers can refer to Ref. 7. For isotropic scattering, $\Phi(\Omega'\to\Omega)=1$, thus, the integration in Eq. (5) vanishes and there is

$$G(\boldsymbol{r},\Omega) = -[1/(\kappa+\sigma)](\Phi\cdot\nabla)F(\boldsymbol{r},\Omega) \tag{7}$$

Substituting the variable G in Eq. (6) with Eq. (7), the EPF of the RTE is then obtained as

$$(\Omega\cdot\nabla)\frac{1}{\kappa+\sigma}(\Omega\cdot\nabla)F(\boldsymbol{r},\Omega) = (\kappa+\sigma)F(\boldsymbol{r},\Omega) - 2\kappa I_b(\boldsymbol{r}) - \frac{\sigma}{4\pi}\int_{\Omega'=2\pi} 2F(\boldsymbol{r},\Omega')\,\mathrm{d}\Omega' \tag{8}$$

Equation (8) is a second-order equation that has been shown to be positive definite and self adjoint.[8] Similarly, by manipulating Eqs. (3), (4), and (7), the radiative boundary condition for Eq. (2a) can also be derived in terms of the variable F as

$$\frac{(\boldsymbol{n}\cdot\Omega)}{\left|\boldsymbol{n}\cdot\Omega\right|}\frac{1}{\kappa+\sigma}(\Omega\cdot\nabla)F(\boldsymbol{r}_w,\Omega) = F(\boldsymbol{r}_w,\Omega) - 2\varepsilon I_b(\boldsymbol{r}_w) - \frac{2(1-\varepsilon)}{\pi}q(\boldsymbol{r}_w) \tag{9}$$

In the derivation of Eq. (9), care should be taken to determine the sign of the term

$$[1/(\kappa + \sigma)](\Omega \cdot \nabla)F(\boldsymbol{r}_w, \Omega)$$

which is dependent on the cosine value of the angle between $\boldsymbol{n}$ and Ω.

Equations (8) and (9) represent the vector forms of the RTE and they can be transformed into the equations in terms of x and y variables by substituting each vector with its vector components and executing the vector operators:

$$\frac{\partial}{\partial x}\left[\frac{1}{\kappa+\sigma}\left(\mu^2\frac{\partial F}{\partial x}+\mu\xi\frac{\partial F}{\partial y}\right)\right] + \frac{\partial}{\partial y}\left[\frac{1}{\kappa+\sigma}\left(\mu\xi\frac{\partial F}{\partial x}+\xi^2\frac{\partial F}{\partial y}\right)\right] = (\kappa+\sigma)F - 2\kappa I_b - \frac{\sigma}{4\pi}\int_{\Omega'=2\pi} 2F\,\mathrm{d}\Omega' \tag{10}$$

$$\frac{(\mu n_x + \xi n_y)}{|\mu n_x + \xi n_y|}\frac{1}{\kappa+\sigma}\left(\mu\frac{\partial F}{\partial x}+\xi\frac{\partial F}{\partial y}\right) = F - 2\varepsilon I_b - \frac{2(1-\varepsilon)}{\pi}q \tag{11}$$

where n_x and n_y denote the wall normal vector components whose values are different at different walls.

Numerical Analysis

Discrete Ordinates Equations

The EPF of RTE, Eq. (10), involves not only spatial differentiation, but also the angular integration over the solid angle Ω. To solve this equation numerically, the angular dependence is first removed. In the DOM, the RTE is replaced by a set of equations for a finite number of M ordinate directions. For a specific ordinate direction m, defined by $\Omega_m = (\mu_m, \xi_m)$, the integral in Eq. (10) is replaced by a quadrature of order M with the appropriate angular weights w_m

$$\frac{\partial}{\partial x}\left[\frac{1}{\kappa+\sigma}\left(\mu_m^2\frac{\partial F^m}{\partial x}+\mu_m\xi_m\frac{\partial F^m}{\partial y}\right)\right] + \frac{\partial}{\partial y}\left[\frac{1}{\kappa+\sigma}\left(\mu_m\xi_m\frac{\partial F^m}{\partial x}+\xi_m^2\frac{\partial F^m}{\partial y}\right)\right] = (\kappa+\sigma)F^m - 2\kappa I_b - \frac{\sigma}{4\pi}\sum_{m'=1}^{M} 2w_{m'}F^{m'} \tag{12}$$

Since the integration in the even parity RTE is made over 2π solid angles, it is necessary to solve the equations for only half of the directions that would be required if the conventional RTE were applied. The selection of the direction cosines and corresponding weights, that is, the quadrature scheme, is arbitrary, although restrictions arise from the need to preserve symmetries and invariance properties of the physical system. In this study, the level symmetric S_n quadrature scheme[9] was employed.

For the discrete direction Ω_m, the radiative boundary condition for Eq. (12) can be written as

$$\frac{(\mu_m n_x + \xi_m n_y)}{|\mu_m n_x + \xi_m n_y|}\frac{1}{\kappa+\sigma}\left(\mu_m\frac{\partial F^m}{\partial x}+\xi_m\frac{\partial F^m}{\partial y}\right) = F^m - 2\varepsilon I_b - \frac{2(1-\varepsilon)}{\pi}q \tag{13}$$

Equation (13) also involves the angular integration that is implicitly included in the calculation of q.

Spatial Discretization

To solve the discrete ordinates equation, the rectangular enclosure is subdivided into small control volumes by $MX \times MY$ meshes. Within each control volume, the spatially discretized equation for the variable F in Ω_m is derived. Since Eq. (12) is similar to the transport equations in fluid dynamics, it can be discretized spatially in the same way as in computational fluid dynamics (CFD).[10] In a control volume, the second-order spatial derivative terms in Eq. (12) are discretized using the second-order central difference scheme, whereas the terms in the right-hand side of Eq. (12) are treated as source terms. The discretized terms are divided into nonmixed-derivative and mixed-derivative parts. The nonmixed-derivative terms are treated implicitly and the mixed-derivative terms are lumped into the explicit part of the source terms. This arrangement reduces the computer memory requirements compared to the fully implicit treatment. For simplicity, only the spatial derivative term in the x direction is presented:

$$\frac{\partial}{\partial x}\left[\frac{1}{\kappa+\sigma}\left(\mu_m^2\frac{\partial F^m}{\partial x}+\mu_m\xi_m\frac{\partial F^m}{\partial y}\right)\right] = \frac{1}{\Delta x_{i,j}}\left[\frac{1}{\kappa+\sigma}\left(\mu_m^2\frac{\partial F^m}{\partial x}+\mu_m\xi_m\frac{\partial F^m}{\partial y}\right)\right]_{i+1/2,j} - \frac{1}{\Delta x_{i,j}}\left[\frac{1}{\kappa+\sigma}\left(\mu_m^2\frac{\partial F^m}{\partial x}+\mu_m\xi_m\frac{\partial F^m}{\partial y}\right)\right]_{i-1/2,j} \tag{14}$$

where i and j represent volume index numbers in the x and y directions, respectively; the terms associated with $\partial F^m/\partial x$ are the nonmixed-derivative terms and the terms involving $\partial F^m/\partial y$ represent the mixed-derivative terms. The nonmixed- and mixed-derivative terms on the $i + \frac{1}{2}$ control volume interface can be written as

$$\frac{1}{\Delta x_{i,j}}\left[\frac{1}{\kappa+\sigma}\left(\mu_m^2\frac{\partial F^m}{\partial x}\right)\right]_{i+1/2,j} = \frac{1}{\Delta x_{i,j}\Delta x_{i+1/2,j}}\left(\frac{\mu_m^2}{\kappa+\sigma}\right)_{i+1/2,j}(F^m_{i+1,j} - F^m_{i,j}) \tag{15}$$

$$\frac{1}{\Delta x_{i,j}}\left[\frac{1}{\kappa+\sigma}\left(\mu_m\xi_m\frac{\partial F^m}{\partial y}\right)\right]_{i+1/2,j} = \frac{1}{4\Delta x_{i,j}\Delta y_{i,j}} \times \left(\frac{\mu_m^2}{\kappa+\sigma}\right)_{i+1/2,j}(F^m_{i+1,j+1} + F^m_{i,j+1} - F^m_{i+1,j-1} - F^m_{i,j-1}) \tag{16}$$

Discretization of the radiative boundary condition, Eq. (13), requires special attention because it is a first-order differential equation and is likely to induce instability in the numerical procedure.[6,10] To overcome this problem, an upwind scheme is used. The order of an upwind scheme is selected to be second- or third-order to be compatible with the scheme used for the interior control volume. For simplicity, only the first-order spatial derivative term in the x direction is presented:

$$\frac{(\mu_m n_x + \xi_m n_y)}{|\mu_m n_x + \xi_m n_y|}\frac{\mu_m}{\kappa+\sigma}\frac{\partial F^m}{\partial x} = -\frac{1}{\Delta x_{i,j}}[(f_{i+1/2,j} - f_{i-1/2,j}) - (d_{i+1/2,j} - d_{i-1/2,j})] \tag{17}$$

The first term on the right-hand side of Eq. (17) denotes a first-order upwind scheme and the second term represents a higher-order antidiffusion correction:

$$f_{i+1/2,j} = \max[0, \quad \theta]F^m_{i,j} - \max[0, \quad -\theta]F^m_{i+1,j}$$

$$f_{i-1/2,j} = \max[0, \quad \theta]F^m_{i-1,j} - \max[0, \quad -\theta]F^m_{i,j}$$

where the variable θ is given as

$$\theta = -\frac{(\mu_m n_x + \xi_m n_y)}{|\mu_m n_x + \xi_m n_y|}\frac{\mu_m}{\kappa + \sigma}$$

and the second- or third-order antidiffusion term can be written in the following form:

Second-order upwind scheme:

$$d_{i+1/2,j} = \tfrac{1}{2}|\theta|\begin{bmatrix}\Delta F^m_{i-1/2,j}, & \theta > 0\\ \Delta F^m_{i+3/2,j}, & \theta < 0\end{bmatrix}$$

$$d_{i-1/2,j} = \tfrac{1}{2}|\theta|\begin{bmatrix}\Delta F^m_{i-3/2,j}, & \theta > 0\\ \Delta F^m_{i+1/2,j}, & \theta < 0\end{bmatrix}$$

Third-order upwind scheme:

$$d_{i+1/2,j} = \tfrac{1}{2}|\theta|\begin{bmatrix}\frac{2}{3}\Delta F^m_{i+1/2,j} + \frac{1}{3}\Delta F^m_{i-1/2,j}, & \theta > 0\\ \frac{2}{3}\Delta F^m_{i+1/2,j} + \frac{1}{3}\Delta F^m_{i+3/2,j}, & \theta < 0\end{bmatrix}$$

$$d_{i-1/2,j} = \tfrac{1}{2}|\theta|\begin{bmatrix}\frac{2}{3}\Delta F^m_{i-1/2,j} + \frac{1}{3}\Delta F^m_{i-3/2,j}, & \theta > 0\\ \frac{2}{3}\Delta F^m_{i-1/2,j} + \frac{1}{3}\Delta F^m_{i+1/2,j}, & \theta < 0\end{bmatrix}$$

Second-order central scheme:

$$d_{i+1/2,j} = \tfrac{1}{2}|\theta|\Delta F^m_{i+1/2,j} \qquad d_{i-1/2,j} = \tfrac{1}{2}|\theta|\Delta F^m_{i-1/2,j}$$

where ΔF represents central difference with F

$$\Delta F^m_{i+1/2,j} = (F^m_{i+1,j} - F^m_{i,j})/\Delta x_{i+1/2,j}$$

If the index number of the variable F is less than the minimal number 1 or greater than MX, then the index number is taken to be 1 or MX, respectively.

Solution Method

The preceding spatial discretization is carried out in one discrete direction. The same discretization procedure is applied to all M discrete directions. This forms M systems of nonsymmetric algebraic equations. In this study, each direction is solved independently. Before the solution procedure begins, the temperature and partial pressure of the radiatively participating medium in each control volume are provided, and the absorption and scattering coefficients are calculated. Because of the dependence of the source terms and the boundary conditions on the variable F, global iterations are necessary. As the first step of a solution procedure, an initial solution is assumed and used to calculate the variable G from Eq. (7) and intensities from Eq. (3) and Eq. (4). Then the source terms and irradiation are calculated and a system of equations for each direction is solved. The new solution replaces the previous solution and the iterative procedure continues until convergence is obtained.

The solver of the discretized equations is directly from a general CFD code: the FDNS code.[11,12] This matrix solver is based on the preconditioned conjugate gradients squared (CGS) method. Langtangen[13] compared several conjugate gradients methods with preconditioning for nonsymmetric matrix systems with arbitrary sparsity patterns and found that the preconditioned CGS method turned out to be the best method. Incomplete factorization[14] is used as the preconditioner because it is easy to program and has a fast convergence rate.

Results and Discussion

Based on the theoretical and numerical analyses described earlier, a computer program has been developed that can simulate two-dimensional radiation using the EPF. To examine the accuracy and computational efficiency of the EPF of the DOM, another computer program has also been developed that uses the conventional DOM with the step spatial differencing scheme to simulate radiative heat transfer. In this study, the solution from the EPF of the DOM is termed the even parity solution and the solution from the conventional DOM is termed the discrete ordinates solution. The geometry studied in this paper is the two-dimensional square enclosure with both L and H equal to unity (Fig. 1). For this geometry, three kinds of problems were selected: 1) an absorbing–emitting medium in a black enclosure, 2) a purely scattering medium in a black or gray enclosure, and 3) an absorbing–emitting medium with a uniform heat source in a black enclosure. These three problems have been considered previously,[3–5] and the exact or accurate zone solutions are available and they are presented for comparison in addition to the even parity solution and discrete ordinates solution.

In each even parity solution, the level symmetric S_8 quadrature scheme[9] is applied, and the spatial grid mesh used is 20 $\times$ 20 and it is clustered in the regions near the walls. A uniform grid mesh should be avoided in the even parity solution because the radiative wall flux, one of the major quantities of interest, is a function of the gradient of the variable F, which usually changes rapidly near the wall. Convergence is measured using a tolerance in the incident radiation. Iterations are continued until the relative incident radiation change is less than a preselected tolerance in each surface or volume element. Unless otherwise specified, the preselected tolerance in this study is 0.01%, which is small enough for most problems. However, for a problem with strongly reflecting walls, a smaller convergence tolerance may have to be used. Otherwise, sizable errors can be found in the results. This is discussed in one of the problems considered later. All computation was conducted on the IBM RISC/6000 machine. For a combustion problem, the radiative transfer quantities of interest are the net radiative wall flux and the radiative divergence. In this study, however, the incident radiation or the emissive power, which is the derivative quantity of the radiative divergence, is used to show the accuracy of the radiative divergence.

The discrete ordinates solution for each problem was obtained based on the same conditions as those in the even parity solution for the convenience of comparison. It should be noted that the use of nonuniform grid mesh is not necessary in the discrete ordinates solution. This is different from the even parity solution.

Absorbing–Emitting Medium in a Black Enclosure

The first problem examined is an enclosure with cold, black walls and a purely absorbing–emitting medium maintained at

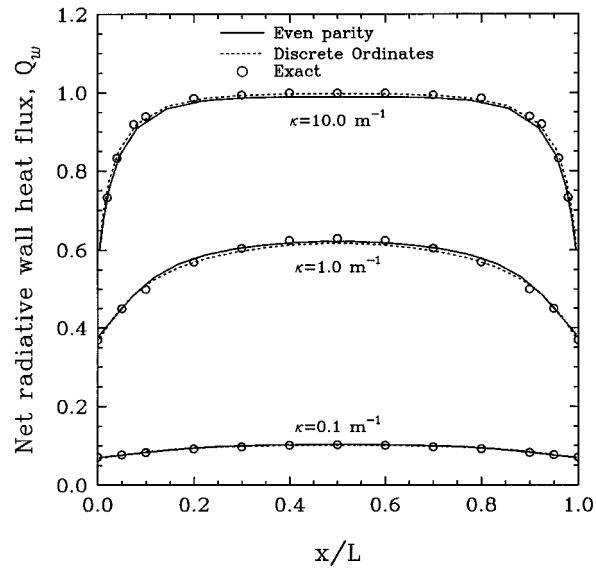

Fig. 2 Comparison of net radiative wall heat flux for different absorption coefficients.

Table 1 CPU time and iterations for the first problem

	CPU time, s		Iterations	
κ	Even parity	Discrete ordinates	Even parity	Discrete ordinates
0.1	95.97	2.54	96	2
1.0	27.85	2.15	32	2
10.0	16.61	2.16	22	2

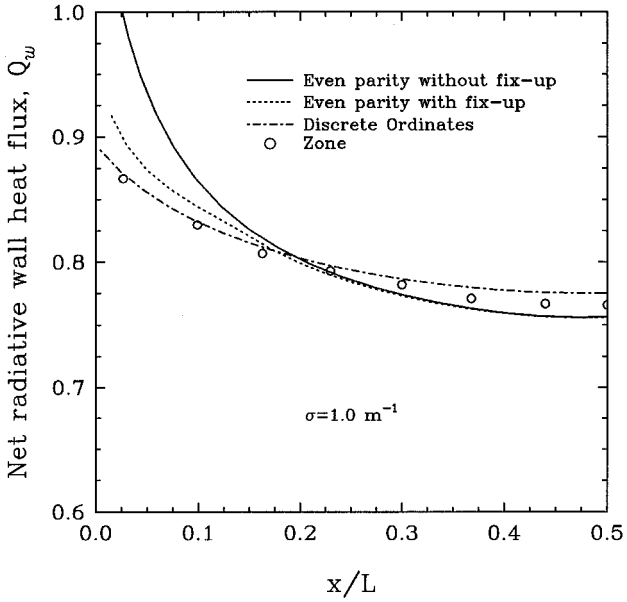

Fig. 3 Comparison of net radiative wall heat flux.

an emissive power of unity. The selected medium κ varies from 0.1 to 1.0 to 10.0. This benchmark problem is studied frequently because an exact solution[15,16] for net radiative wall flux is available.

Figure 2 shows comparisons of the net radiative wall flux among the even parity, discrete ordinates, and exact solutions at κ of 0.1, 1.0, and 10.0. As κ increases, the walls receive more radiative energy and net radiative wall flux distribution is seen to become smoother in the central region and steeper in the near-wall regions. At each κ, the prediction from the even parity solution is found to be essentially coincident with the discrete ordinates and exact solutions in the all regions and the maximum difference are within 2%. Fiveland and Jessee[4,5] investigated the same problem using the finite element formulation of the even parity RTE and found the accuracy of the even parity solutions degraded as κ increased when a uniform grid mesh was applied. This degradation should disappear if a nonuniform and fine grid mesh is used.

The required CPU time and iterations for the even parity and discrete ordinates solutions are listed in Table 1. In the discrete ordinates solution, the source terms in the discretized equations and boundary conditions are independent of the intensity. Therefore, only two iterations are required to obtain convergent solutions at each κ. However, in the even parity solution, there exist the mixed derivative terms [see Eq. (14)] in the discretized equations, even for a simple rectangular geometry. This results in a strong dependence of the source terms on the variable F. Thus, the CPU time and iteration number are seen considerably higher in the even parity solution, especially for the case with a small optical thickness.

Purely Scattering Medium in a Black or Gray Enclosure

The second problem examined is an isotropically scattering medium in a black or gray enclosure. The coefficient σ is 1.0. The lower wall (wall 3 as shown in Fig. 1) is a hot wall and it has an emissive power of unity, whereas the rest are cold walls. Several methods have been used to solve this problem. The solution from the zone method[17,18] has been considered to be accurate. Thus, the even parity solution will be tested against the zone solution as well as the discrete ordinates solution at different wall emissivities.

Unlike the previous problem, the present problem has discontinuous emissive power at the lower left and right corners. As indicated by Ratzel and Howell,[18] the second-order central difference scheme seems to have difficulty in capturing all of the physics in the corner regions with strong emissive power discontinuities. One example is the case considered here for a black enclosure where the hot wall infinitesimally near the corner is emitting and absorbing and the cold side walls infinitesimally near the corner are only absorbing. In this case, the net radiative wall heat flux on the hot wall from the even parity solution is found to be overestimated in the corner regions as shown in Fig. 3. A further check of other radiative quantities indicates that radiative intensities become negative at some

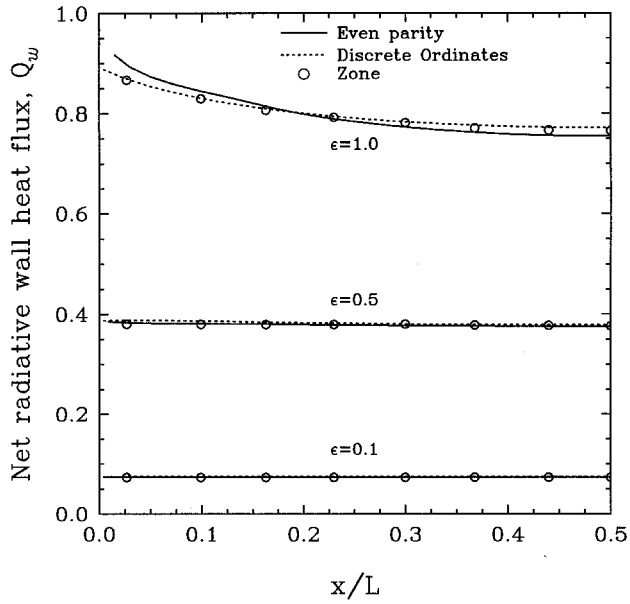

Fig. 4 Comparison of net radiative wall heat flux for different wall emissivities.

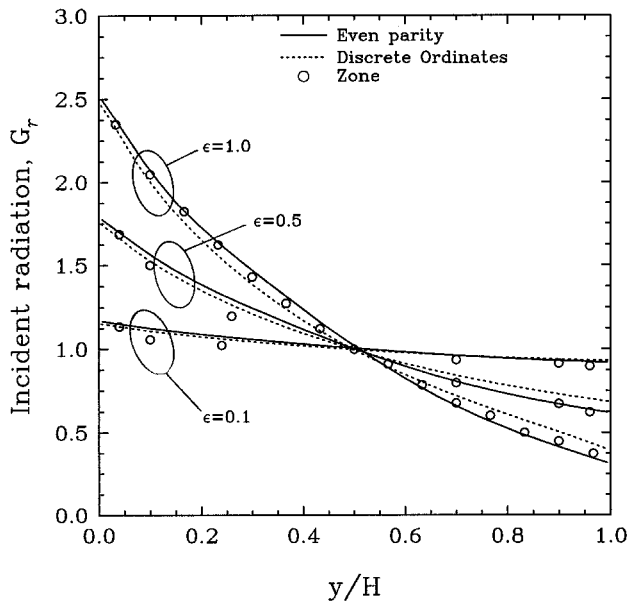

Fig. 5 Comparison of centerline incident radiation for different wall emissivities.

points near the corner regions. The regions with negative intensity are smaller, and the radiative wall flux is less overestimated in the corner regions as the grid mesh becomes finer. However, it is very difficult to completely avoid negative intensities unless a prohibitively fine grid mesh is used. This finding is contrary to the common belief that EPF ensures positive intensities.[3–5] Therefore, although the variable F is always positive, the radiative intensity, which is a function of the variable F, can become negative for some special cases. This is an important observation in this study.

Physically unrealistic negative intensities result in an incorrect prediction of radiative wall heat flux and they should be avoided. In this study, the negative intensities are avoided by using the same negative intensity fix-up procedure as that in the conventional DOM. That is, when a negative intensity is encountered, it is set to be zero. The corresponding variable F is then calculated from Eqs. (3) and (4) rather than solved from the EPF. With this procedure, the even parity results in radiative wall heat flux in the corner regions drop considerably, as seen in Fig. 3, and their difference from the zone solution is narrowed within 4%. This reasonable solution will be used for comparison with the discrete ordinates and zone solutions in the following figures. For some gray enclosures such as those to be considered in Figs. 4 and 5, the corner emissive power discontinuity is less critical because the cold walls can also reflect incident radiation, and therefore, the previous negative intensity fix-up procedure is not necessary.

Figure 4 shows the net radiative wall flux on the hot wall for even parity solutions compared to the discrete ordinates and zone solutions for enclosures with wall emissivities of 1.0, 0.5, and 0.1. Three different solutions are seen to have very good agreement in each case. For a problem with strongly reflecting walls, the incident radiation change between two consecutive iterations becomes very small in the iterative solution procedure in the even parity solution. Hence, the preselected convergence tolerance should be small enough to guarantee that the final solution is really convergent. Otherwise, gradually increased errors will be found in the solution as the wall emissivities are decreased. Several different tolerances were used to test the convergence for the two gray enclosures. The solutions were considered to be convergent only when the preselected tolerance was less than 0.001%. Therefore, the even parity solutions for the two gray enclosures in Fig. 4 were obtained using a tolerance one order of magnitude less than other problems.

Comparisons of centerline incident radiation distributions for the three cases considered in Fig. 4 are demonstrated in Fig. 5. Each even parity solution is seen to compare very well with the discrete ordinates and zone solutions. At the point of $x/L = 0.5$ and $y/H = 0.5$, all solutions predict an incident radiation of unity that matches the exact solution.[19]

Table 2 CPU time and iterations for the second problem

		CPU time, s		Iterations	
σ	ε	Even parity	Discrete ordinates	Even parity	Discrete ordinates
1.0	1.0	41.77	5.74	47	8
1.0	0.5	94.66	14.20	132	19
1.0	0.1	434.14	59.70	552	82
0.1	1.0	139.69	3.01	154	4
10.0	1.0	44.60	39.00	63	55
100.0	1.0	172.37	328.79	241	425

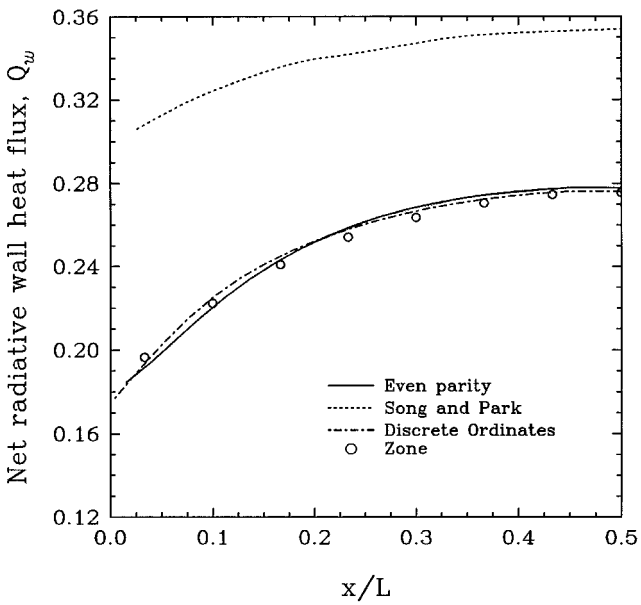

Fig. 6 Comparison of net radiative wall heat flux at $\kappa = 0.1$ m^{-1}.

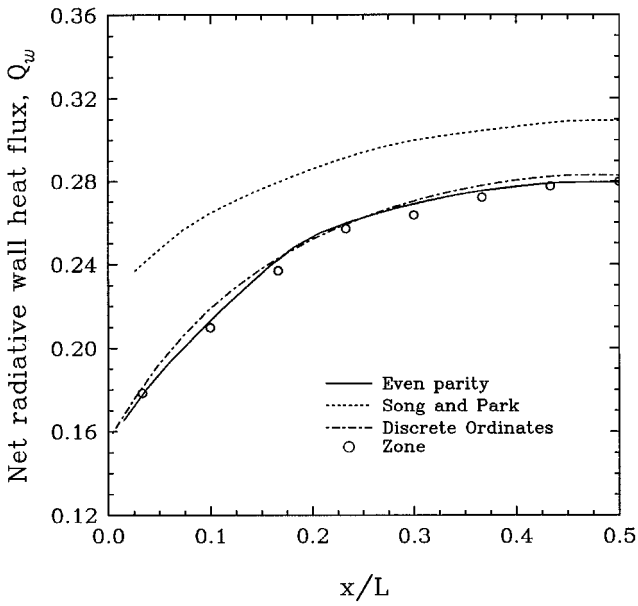

Fig. 7 Comparison of net radiative wall heat flux at $\kappa = 1.0$ m^{-1}.

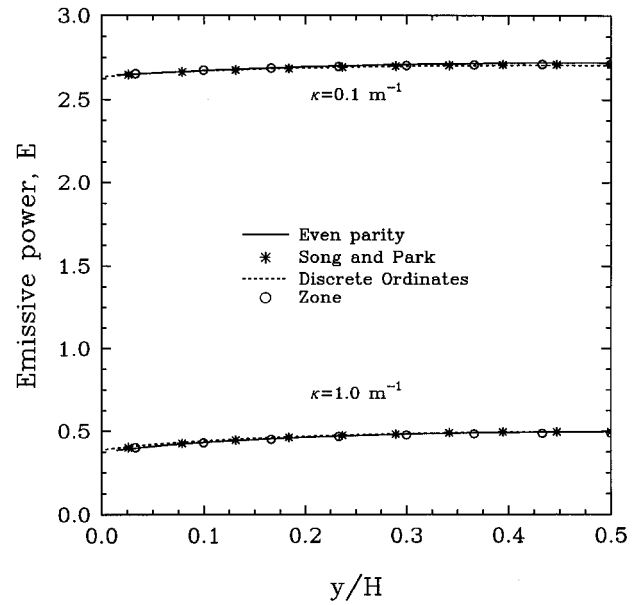

Fig. 8 Comparison of centerline ($x/L = 0.5$) emissive power distributions.

Table 3 CPU time and iterations for the third problem

	CPU time, s		Iterations	
κ	Even parity	Discrete ordinates	Even parity	Discrete ordinates
0.1	88.31	4.41	93	6
1.0	28.17	10.22	33	14
10.0	95.64	80.16	124	111

Table 2 shows the CPU time and iterations for the even parity and discrete ordinates solutions. With a decrease of wall emissivity, the convergence in both the even parity and discrete ordinates solutions becomes slow. However, the discrete ordinate solution still converges six to seven times faster than the even parity solution for each case. To examine the convergence characteristics for different optical thicknesses, three additional cases with σ equal to 0.1, 10.0, and 100.0 in a black enclosure were considered and the corresponding CPU time and iterations are listed in Table 2. As the optical thickness increases, the number of iterations rises steadily for the discrete ordinates solution, but falls at first and then rises for the even parity solution. Except for the case with a very large optical thickness, the convergence in the discrete ordinate solution appears faster than the even parity solution.

Absorbing–Emitting Medium with a Uniform Heat Source in a Black Enclosure

The third problem examined is an enclosure that has a uniform heat source with a value of unity. The walls are assumed to be cold and black. The medium is purely absorbing–emitting and it has κ equal to 0.1 or 1.0. Because of the internal heat source, this problem requires an iterative solution procedure with the energy equation. Similar to the second problem, the accurate zone solution[3,18] is available for this problem and it will be used to validate the even parity solution.

Figures 6 and 7 present the net radiative wall flux distributions at κ of 0.1 and 1.0, respectively. At each case, the even parity solution demonstrates very good agreement with the discrete ordinates and zone solutions and the maximum difference among three solutions is less than 1%. Song and Park[3] investigated the same problem using the EPF and their results differ significantly from the zone solution as shown in the figures. One possible reason for such large discrepancies is that they solved the even parity RTE based on a uniform grid mesh that can not resolve radiation accurately at the boundaries.

The emissive power distributions at the center location $x/L = 0.5$, with κ equal to 0.1 and 1.0, are plotted in Fig. 8. In contrast to the net radiative wall flux in Figs. 6 and 7, very good agreement is seen for all different solutions, even for that from Song and Park.[3] Thus, it is concluded that the results predicted by the even-parity RTE is less susceptible to grid mesh inside the medium. Such a fact was also reported by Fiveland and Jessee.[4,5]

The CPU time and iterations for the even parity and discrete ordinates solutions are presented in Table 3. To investigate the convergence characteristics for different optical thicknesses, an additional case with κ equal to 10.0 was considered and the corresponding CPU time and iterations are also listed in Table 3. Similar to the second problem, the discrete ordinates solution converges slowly, whereas the even parity solution converges fast first and then slowly as the optical thickness increases. For each case, the discrete ordinates solution needs less CPU time and iterations than the even parity solution, especially for a small optical thickness.

Conclusions

The EPF of the DOM has been employed to investigate radiative heat transfer in two-dimensional enclosures containing an absorbing–emitting and scattering medium. Compared to the conventional RTE, a finer grid mesh and a smaller convergence tolerance have to be used in the numerical treatment of the EPF. For a problem with a strong corner emissive power discontinuity, the EPF cannot ensure positive radiative intensities and the negative intensity fix-up procedure should be used to reduce the related side effects. For an absorbing–emitting and isotropically scattering medium, although radiation from the EPF of the DOM only needs to be simulated in the half of the angular domain that would be required if the conventional RTE were applied, the even parity solution usually requires more CPU time and iterations to converge in comparison with the conventional DOM, especially for the case with a small optical thickness. From the present study, it appears that the conventional DOM is more robust than the EPF of the DOM. More work is needed to examine this claim for the more complicated problems in the future.

Acknowledgments

Partial support for J. Liu, H. M. Shang, and Y. S. Chen through Contract NAS8-40582 from the NASA Long Term/ High Payoff technologies program to Engineering Sciences, Inc., is greatly appreciated.

References

[1]Viskanta, R., and Menguc, M. P., "Radiation Heat Transfer in Combustion Systems," *Progress in Energy and Combustion Science*, Vol. 13, No. 2, 1987, pp. 97–160.

[2]Lewis, E. E., and Miller, W. F., *Computational Methods of Neutron Transport*, Wiley, New York, 1984.

[3]Song, T. H., and Park, C. W., "Formulation and Application of the Second Order Discrete Ordinate Method," *Transport Phenomena Science and Technology 1992*, edited by B.-X. Wang, Higher Education Press, Beijing, PRC, 1992, pp. 833–841.

[4]Fiveland, W. A., and Jessee, J. P., "Finite Element Formulations of the Discrete-Ordinates Method for Multidimensional Geometries," *Journal of Thermophysics and Heat Transfer*, Vol. 8, No. 3, 1994, pp. 426–433.

[5]Fiveland, W. A., and Jessee, J. P., "Comparison of Discrete Ordinates Formulations for Radiative Heat Transfer in Multidimensional Geometries," *Journal of Thermophysics and Heat Transfer*, Vol. 9, No. 1, 1995, pp. 47–54.

[6]Koch, R., Krebs, W., Wittig, S., and Viskanta, R., "A Parabolic Formulation of the Discretes Ordinates Method for the Treatment of Complex Geometries," International Symposium on Radiative Transfer, Kusadasi, Turkey, Aug. 1995.

[7]Lillie, R. A., and Robinson, J. C., "A Linear Triangle Finite Element Formulation for Multigroup Neutron Transport Analysis with Anisotropic Scattering," Oak Ridge National Lab., TM-5281, 1976.

[8]Kaplan, S., and Davis, J. A., "Canonical and Involuntary Transformations of the Variational Problems of Transport Theory," *Nuclear Science and Engineering*, Vol. 28, No. 1, 1967, pp. 166, 167.

[9]Fiveland, W. A., "Three-Dimensional Radiative Heat Transfer Solutions by the Discrete-Ordinates Method," *Journal of Thermophysics and Heat Transfer*, Vol. 2, No. 4, 1988, pp. 309–316.

[10]Hirsch, C., *Numerical Computation of Internal and External Flows*, Vol. 2, Wiley, New York, 1990.

[11]Chen, Y. S., "Compressible and Incompressible Flow Computations with a Pressure Based Method," AIAA Paper 89-0286, Jan. 1989.

[12]Wang, T. S., and Chen, Y. S., "Unified Navier-Stokes Flowfield and Performance Analysis of Liquid Rocket Engines," *Journal of Propulsion and Power*, Vol. 9, No. 5, 1993, pp. 678–685.

[13]Langtangen, H. P., "Conjugate Gradient Methods and ILU Preconditioning of Non-Symmetric Matrix Systems with Arbitrary Sparsity Patterns," *International Journal for Numerical Methods in Fluid*, Vol. 9, No. 2, 1989, pp. 213–233.

[14]Dupont, T., Kendall, R. P., and Rachford, M. M., "An Approximate Factorization Procedure for Solving Self-Adjoint Elliptic Difference Equations," *SIAM Journal of Numerical Analysis*, Vol. 5, No. 3, 1968, pp. 559–573.

[15]Fiveland, W. A., "Discrete-Ordinates Solutions of the Radiative Transport Equation for Rectangular Enclosures," *Journal of Heat*

Transfer, Vol. 106, No. 4, 1984, pp. 699–706.

[16]Shah, N., "New Method of Computation of Radiation Heat Transfer in Combustion Chambers," Ph.D. Dissertation, Dept. of Mechanical Engineering, Imperial College of Science and Technology, Univ. of London, London, 1979.

[17]Sanchez, A. A., Krajewski, W. F., and Smith, T. F., "A General Radiative Transfer Model for Atmospheric Remote Sensing Studies in Multi-Dimensional Media," Iowa Inst. of Hydraulic Research, Rept. 355, Iowa City, IA, Jan. 1992.

[18]Ratzel, A. C., and Howell, J. R., "Two-Dimensional Radiation in Absorbing-Emitting Media Using the P-N Approximation," *Journal of Heat Transfer*, Vol. 105, No. 2, 1983, pp. 333–340.

[19]Crosbie, A. I., and Schrenker, R. G., "Exact Expressions for Radiative Transfer in a Three-Dimensional Rectangular Geometry," *Journal of Quantitative Spectroscopy and Radiative Transfer*, Vol. 28, No. 6, 1982, pp. 507–526.